



Published in final edited form as:

J Am Chem Soc. 2019 June 05; 141(22): 8798–8806. doi:10.1021/jacs.9b00045.

Discovery of FAHFA-containing Triacylglycerols and Their Metabolic Regulation

Dan Tan¹, Meric Erikci Ertunc^{1,‡}, Srihari Konduri^{2,‡}, Justin Zhang², Antonio M. Pinto¹, Qian Chu¹, Barbara B. Kahn³, Dionicio Siegel^{2,*}, Alan Saghatelian^{1,*}

¹Clayton Foundation Laboratories for Peptide Biology, Salk Institute for Biological Studies, 10010 North Torrey Pines Road, La Jolla, CA 92037-1002, United States

²Skaggs School of Pharmacy and Pharmaceutical Sciences, University of California-San Diego, 9500 Gilman Drive, La Jolla, California 92093-0934, United States

³Division of Endocrinology, Diabetes and Metabolism, Department of Medicine, Beth Israel Deaconess Medical Center, Harvard Medical School, Boston, Massachusetts 02215, United States

Abstract

FAHFAs are a class of bioactive lipids which show great promise for treating diabetes and inflammatory diseases. Deciphering the metabolic pathways that regulate endogenous FAHFA levels is critical for developing diagnostic and therapeutic strategies. However, it remains unclear how FAHFAs are metabolized in cells or tissues. Here, we investigate whether FAHFAs can be incorporated into other lipid classes and identify a novel class of endogenous lipids, FAHFA-containing triacylglycerols (FAHFA-TGs), which contain a FAHFA group esterified to the glycerol backbone. Isotope-labeled FAHFAs are incorporated into FAHFA-TGs when added to differentiated adipocytes which implies the existence of enzymes and metabolic pathways capable of synthesizing these lipids. Induction of lipolysis (i.e., triacylglycerol hydrolysis) in adipocytes is associated with marked increases in nonesterified FAHFA levels demonstrating that FAHFA-TGs breakdown is a regulator of cellular FAHFA levels. To quantify FAHFA levels in FAHFA-TGs and determine their regioisomeric distributions, we developed a mild alkaline hydrolysis method that liberates FAHFAs from triacylglycerols for easier detection. FAHFA-TG concentrations are greater than 100-fold than that of nonesterified FAHFAs, indicating that FAHFA-TGs are a major reservoir of FAHFAs in cells and tissues. The discovery of FAHFA-TGs reveals a new branch of TG and FAHFA metabolism with potential roles in metabolic health and regulation of inflammation.

Graphical Abstract

*Corresponding Author drsiegel@ucsd.edu and asaghatelian@salk.edu.

‡M.E.E. and S.K. contributed equally.

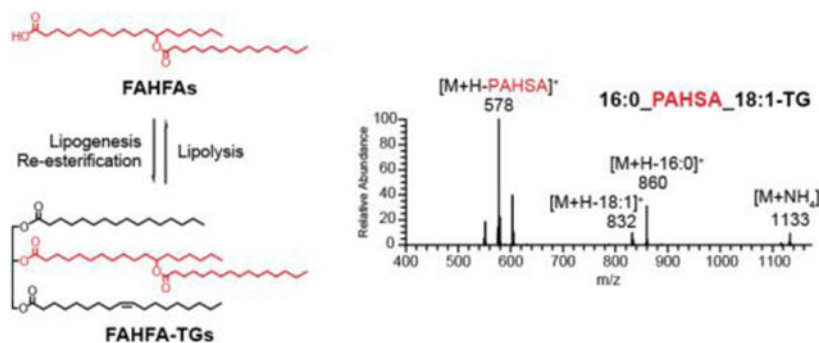
ASSOCIATED CONTENT

Supporting Information

The Supporting Information is available free of charge on the ACS Publications website.

Supplementary figures, detailed description of synthetic procedures and spectral data for FAHFA-TGs and FAHFA-CE (PDF)

The authors declare no competing financial interest.



INTRODUCTION

FAHFAs (Fatty Acid esters of Hydroxy Fatty Acids) are a recently discovered class of lipids that are highly elevated in the adipose tissue of transgenic mice overexpressing glucose transporter 4 (GLUT4) selectively in their adipose tissue (AG4OX mice)^{1–3}. FAHFAs are grouped into families based on the composition of their acyl chains, and each family contains multiple regioisomers that differ in position of the ester bond that links the acyl chains². Since their initial discovery, many FAHFAs have been identified in plants and animals^{2,4–7}. Oral administration of 5- and 9- PAHSA (palmitic acid ester of hydroxy stearic acid), two of the most up-regulated FAHFA species in AG₄OX mice, reduces blood glucose levels and improves insulin sensitivity in mice^{2,8}. Analysis of serum and adipose tissue PAHSA levels in people that differ in their insulin sensitivity revealed that multiple PAHSA regioisomers correlate highly with insulin sensitivity², with lower FAHFA levels observed in insulin resistant individuals. FAHFAs also exhibit anti-inflammatory effects. For example, 9-PAHSA and 13-DHAHLA (docosahexaenoic acid ester of 13-hydroxy linoleic acid, a polyunsaturated FAHFA), inhibit LPS-induced proinflammatory cytokine production in macrophages and dendritic cells^{2,4}. Furthermore, administration of 9-PAHSA to mice on a high-fat diet results in lower levels of inflammatory macrophages in their adipose tissue², and 9-PAHSA treatment in a mouse model of colitis reduces the clinical and pathological disease severity⁹, highlighting a role for FAHFAs as anti-inflammatory lipids.

These findings open up new opportunities of treatment for diabetes and inflammatory diseases, but a deeper understanding of the metabolic pathways regulating endogenous FAHFA levels are needed to proceed with novel diagnostic and therapeutic strategies. Biochemical studies have identified three hydrolases—CEL, AIG1 and ADTRP—as putative FAHFA hydrolases that cleave the FAHFA ester^{10–11}, but the role of these enzymes in FAHFA regulation *in vivo* must still be verified. Recent work has linked antioxidant pathways regulated by nuclear factor (erythroid-derived 2)-like 2 (Nrf2) and peroxiredoxin-6 (PRDX6) to changes in endogenous FAHFA levels⁵, though the exact biochemical mechanism linking these genes to FAHFAs remains enigmatic.

In addition to the synthesis and degradation of FAHFA itself, the presence of a carboxylic acid in FAHFAs raises the possibility that these lipids can be incorporated into other lipid classes, where FAHFA replaces a fatty acid in these structures. We set out to address this question by synthesizing FAHFA-containing lipids, developing assays to detect these lipids,

and testing whether these lipids are present in cells and tissues. We focused on FAHFA-containing triacylglycerols (FAHFA-TGs) and cholesteryl esters (FAHFA-CEs) because TGs are major storage forms of fatty acids in mammalian tissues^{12–13} and TGs and CEs are transported throughout the body in lipoprotein particles¹⁴.

By developing mass spectrometry methods, we detected FAHFAs in TGs, providing the only example of FAHFAs being metabolized through their carboxylates in mammals. FAHFA metabolism appears to be specific, as we did not observe any FAHFAs incorporated into CEs. TGs are depots for fatty acid storage during nutritional rich times and are hydrolyzed to release fatty acids under fasting conditions. The regulated balance of fatty acid esterification and TG hydrolysis provides a buffer system to maintain the physiological fatty acid levels¹⁵. Our data suggests that FAHFA-TGs may serve a similar role in regulating FAHFA levels, and reveals a pathway with potential relevance in the metabolic and inflammatory roles of FAHFAs.

RESULTS AND DISCUSSION

Syntheses of FAHFA-containing triacylglycerols and cholesteryl esters

To test our hypothesis, we synthesized a variety of FAHFA-TGs and a FAHFA-CE. The syntheses of the FAHFA-TGs were achieved through iterative Steglich esterification reactions¹⁶ (Scheme 1). The use of 1-ethyl-3-(3-dimethylaminopropyl)carbodiimide (EDC) over *N,N'*-dicyclohexylcarbodiimide (DCC) greatly simplified purification. The expected reactivity of glycerol allowed sequential esterification of the primary alcohols and lastly coupling of the third acid onto the secondary alcohol. Similar reaction with a single esterification between cholesterol and FAHFA provide the FAHFA-CE standard (Supporting Information). The use of glycerol-D₅ or 9-PAHSA assembled using palmitic acid (U-¹³C₁₆) provided heavy standards using the same synthetic strategy.

Discovery of endogenous FAHFA-TGs

In order to develop workflow for analysis of potential endogenous FAHFA-TGs and FAHFA-CEs, we initially examined the fragmentation rules of synthesized FAHFA-TGs and FAHFA-CEs with high resolution mass spectrometry. A representative MS/MS spectrum of one FAHFA-TG species (16:0/PAHSA/18:1-TG) (Figure 1A) in positive ionization mode has an ion for the ammonium adduct of the intact FAHFA-TG (*m/z* 1133.0421) and ions corresponding to the neutral loss of each fatty acyl chain. The fragmentation pattern we observed for FAHFA-TGs is similar to that of triacylglycerols^{17–18} except that the FAHFA moiety provides two product ions, one resulting from the entire FAHFA and a second from the cleavage of the FAHFA ester bond (Figure 1A). For example, the fragment ion at *m/z* 577.5189 is generated from the loss of the PAHSA moiety, while the ion at *m/z* 603.5344 corresponds to the simultaneous loss of two palmitic acid groups, one from the acyl chain esterified to the glycerol backbone and the other from the PAHSA moiety (Figure 1A). FAHFA-CEs also form ammonium adducts in positive ionization mode. As exemplified by the MS/MS spectrum of OAHSA-CE (Figure S1), the most intense fragment corresponds to the characteristic cholestene cation at *m/z* 369.3505^{18–19}. Also observed are acylium ions from hydroxy stearic acid (*m/z* 283.2622), oleic acid (*m/z* 265.2508), and OAHSA (*m/z*

547.5053). The ion at m/z 565.5176 corresponds to the water adduct of the acylium ion of OAHSA.

We next analyzed the lipid extract from adipose tissue of WT mouse, where highest levels of nonesterified FAHFAs were detected². Using the combination of accurate masses, retention time, and fragmentation behavior, various endogenous FAHFA-TGs were detected, which differ in the FAHFA moiety and the two other fatty acid groups attached to the glycerol backbone. For example, the MS/MS spectrum of the ion at m/z 1133.0417 from the adipose tissue is in agreement with the spectrum of the authentic standard (Figure 1B). The additional fragment ion at m/z 551.5023 is probably derived from the loss of the OAHSA moiety from 16:0/OAHSA/16:0-TG which shares the same mass with 16:0/PAHSA/18:1-TG. In addition, we examined FAHFA-TGs with two FAHFA moieties, FAHFA-containing diacylglycerols, and FAHFA-containing monoacylglycerols, but such species were not detected. Despite our best efforts, we did not detect any FAHFA-CEs in either adipose tissue or liver where CEs are chiefly present, suggesting that FAHFA-CEs are not present or below the detection limit of our methodology. The detection of FAHFA-TGs suggests that FAHFAs can be selectively metabolized into other lipid classes.

Since this is the first report of a FAHFA-TG, we felt it necessary to validate the existence of FAHFA-TGs using an orthogonal method. We used a biochemical approach to isolate the adipose neutral lipid fraction, which should include FAHFA-TGs, from FAHFAs by solid phase extraction. We then hydrolyzed this neutral lipid fraction under mild basic conditions that preferably cleave the ester bonds on the glycerol backbone rather than the ester within the FAHFA moiety. The chemical synthesis of FAHFAs revealed that the FAHFA backbone ester is relatively resistant to hydrolysis, and this knowledge enabled us to use selective hydrolysis to liberate FAHFAs under conditions that should not break down FAHFAs. Using this approach, we detected FAHFAs in the neutral lipid fraction after hydrolysis, but not in unhydrolyzed samples, confirming the existence of FAHFA-TGs in adipose tissue (Figure 1C).

FAHFA-TGs are synthesized from FAHFAs in differentiated adipocytes

To determine whether FAHFA-TGs can be synthesized from FAHFAs in cells, we incubated differentiated 3T3-L1 adipocytes with a ¹³C isotope labeled FAHFA and measured its incorporation into triacylglycerols. The isotope labeled ¹³C-PAHSA provides a unique signal in mass spectra which allows us to measure its incorporation with minimal background noise. We detected various ¹³C-PAHSA-containing triacylglycerol species in lipid extracts from cells treated with ¹³C-PAHSA but not from cells treated with vehicle (Figure 2, Figure S2). Furthermore, we observed an increase in FAHFA-TG levels between 5 and 24 hours (Figure S3), suggesting that once produced, these lipids are fairly stable, providing further support that FAHFA-TGs might be a storage form of FAHFAs.

The acyl CoA:diacylglycerol acyltransferases, DGAT1 and DGAT2, are two key enzymes of triacylglycerol synthesis²⁰. To examine whether they are responsible for FAHFA-TGs synthesis, we co-treated 3T3-L1 adipocytes with ¹³C-PAHSA and DGAT1 or/and DGAT2 inhibitor(s). As shown in Figure 2, inhibiting DGAT1 or DGAT2 alone did not affect the incorporation of ¹³C-PAHSA into triacylglycerols significantly, whereas simultaneous

inhibition of both enzymes significantly reduced the incorporation, suggesting that DGAT1 and DGAT2 may compensate for each other to catalyze FAHFA-TG synthesis, requiring the loss of both activities to observe a change in FAHFA-TG production. We observed that the synthesis was not completely abolished by DGAT1 and DGAT2 inhibition under our experimental conditions. We suspect that the reason for this is our use of low doses of inhibitors (200 nM) to treat the cells because higher doses led to cell death during extended periods (24 hours) in our experiment.

To figure out whether higher doses could have a stronger impact on FAHFA-TG levels, we treated the cells with higher dosage of inhibitors (5 μ M) but shortened the incubation time (3 hours) and avoided killing the cells. Despite the higher doses of inhibitors, FAHFA-TG synthesis was still observed (Figure S4). As a comparison, we examined the effect of DGAT1 and DGAT2 inhibitors under the same conditions on TG synthesis by co-treating the cells with $^{13}\text{C}_{16}$ -palmitic acid and measuring the incorporation of $^{13}\text{C}_{16}$ -palmitic acid into TGs. TG production was inhibited in a dose-dependent manner with 2–8 fold decrease with 5 μ M of inhibitors (Figure S5). To illustrate the difference, if we compare $^{13}\text{C}_{16}$ -PA_18:1_18:1 to $^{13}\text{C}_4$ -PAHSA_18:1_18:1, we observe a ~4-fold reduction in the TG production but only a 1.7-fold reduction in FAHFA-TG levels (Figures S4 and S5). Though more work is necessary to understand the reason that DGAT1/2 inhibition is not completely blocking FAHFA-TG levels, one possible explanation is the existence of additional enzymes that catalyze FAHFA-TG synthesis.

Lipolysis increases nonesterified FAHFA levels

In mammalian cells, lipolysis mediates the breakdown of triacylglycerols to release nonesterified fatty acids, which can be used as fuels to meet energy needs or serve as signaling molecules¹⁵. Adipose triglyceride lipase (ATGL), hormone-sensitive lipase (HSL), and monoacylglycerol lipase (MAGL) are the major enzymes responsible for the three-step triacylglycerol hydrolysis cascade in adipose tissue¹⁵. To test whether FAHFA levels are regulated by this lipolysis pathway, we stimulated lipolysis in 3T3-L1 adipocytes with 3-isobutyl-1-methylxanthine (IBMX) or forskolin (FSK). Under these conditions FAHFA levels increased 1.5–5-fold in adipocytes treated with either of the two lipolysis inducers. Co-culturing the cells with an ATGL inhibitor Atglistatin or an HSL-MAGL dual inhibitor CAY10499 reduced the FAHFA levels augmented by IBMX (Figure 3). We also measured FAHFA levels in conditioned media from these cells and observed similar trends for 12/13-POSHA (Figure S6). The levels of other FAHFA isomers in the medium were too low to be quantified. Our results in 3T3-L1 adipocytes is consistent with the observation that nonesterified FAHFA levels are significantly increased in PG-WAT and SQ-WAT of fasted mice² (Figure S7). These experiments indicate that FAHFA-TG hydrolysis can regulate cellular and extracellular FAHFA levels.

FAHFAs are stored as triacylglycerols in adipose tissue

We next sought to characterize the concentrations of FAHFA-TGs in tissues to determine their potential contribution to overall FAHFA concentrations, which required us to develop a robust method for quantifying FAHFA-TG concentrations. As described above, we utilized an MRM-based method to quantify ^{13}C -PAHSA-containing triacylglycerols in adipocytes.

We treated the cells with heavy labeled PAHSA, which provides unique signals of FAHFA-TGs in mass spectra. However, when we applied the same LC-MS method to measure endogenous FAHFA-TGs in mouse tissues, we observed multiple chromatographic peaks which are not fully resolved. These peaks overlapped with internal standards with similar retention times, masses, and MS/MS spectra. However, the relative intensity of the fragment ions in the MS/MS spectra differed, suggesting a more complex mixture *in vivo*.

By studying the various synthetic FAHFA-TGs, we reasoned that the complexity in the LC-MS chromatograms is at least partially derived from the presence of many isomers which result from the numerous possible combinations of the four fatty acyl chains in a FAHFA-TG molecule. For example, PAHSA/18:1/18:1, POHSA/18:1/18:0, and OAHSA/16:0/18:1 triacylglycerols share the same exact mass, a similar set of fragments, and close retention time on C18 reverse phase. The mixture of the three isomers generated distorted mass traces with different transition ratios compared with each individual standard (Figure S8). This does not even take into account the possibility of different FAHFA regioisomers (e.g. FAHFA-TGs with 9-PAHSA vs 5-PAHSA). We also found that the relative abundance of transitions depends on the position of FAHFA on the glycerol backbone. The loss of FAHFA at sn position is more favorable than FAHFA at sn2 position (Figure S9). Therefore, the intensity change of a transition cannot reflect the abundance change of FAHFA-TG as this can also be caused by the compositional change of positional isomers.

To circumvent this issue and develop a robust method for quantifying FAHFA-TGs, we took advantage of the stability of the internal FAHFA esters to hydrolysis and utilized the aforementioned selective alkaline hydrolysis method to quantify FAHFA-TGs (Figure 4A). We loaded crude lipid extract from adipose tissue onto a silica column, and washed it with 95:5 hexane:ethyl acetate. FAHFAs were still bound to the column due to their high polarity. Neutral lipids were eluted and then hydrolyzed with lithium hydroxide to avoid the hydrolysis of the ester bond within FAHFA. We added a $^{13}\text{C}_{16}$ -PAHSA-containing triacylglycerol during lipid extraction, assuming that the endogenous FAHFA-TGs have similar hydrolysis rate as the internal standard to quantify the FAHFAs in FAHFA-TGs. Considering that the position of FAHFA may affect the hydrolysis rate (i.e. sn1 vs sn2), we performed the experiment twice with two standards separately, $^{13}\text{C}_{16}$ -PAHSA/16:0/16:0-TG (sn1) or 16:0/ $^{13}\text{C}_{16}$ -PAHSA/16:0-TG (sn2). Using this method, we quantified the level of FAHFAs in the triacylglycerol fraction from SQ-WAT of WT mice. Strikingly, the level of FAHFA-TGs, which are represented by the level of esterified FAHFAs, is more than 100-fold greater than that of nonesterified FAHFAs (Figure 4B), confirming that triacylglycerols are a storage form of FAHFAs in adipose tissue. In addition, no obvious difference was observed between sn1 and sn2 standards (Figure 4B).

Regulation of FAHFA-TGs under high fat diet feeding

We next examined the levels of FAHFA-TGs in mice fed with high-fat-diet (HFD). We previously reported that nonesterified PAHSA levels increase in PG-WAT while they decrease in SQ-WAT². By contrast, placing mice on a HFD results in increase in 10-PAHSA and 10-OAHSA or no change in FAHFA-TG levels in both WAT depots. The data support a model of FAHFA-TGs serving as a storage form of FAHFAs under nutrient rich conditions.

The relative abundance of FAHFA regioisomers in FAHFA-TGs is different from what we previously reported for nonesterified FAHFAs in tissues. For example, 9-PAHSA is the most abundant nonesterified PAHSA isomer detected in tissues². However, in the current study we detect 10-PAHSA and 10-OAHSA at the highest levels in FAHFA-TGs from mice on a HFD (Figure 5). We suspected that this is likely due to higher 10-FAHFA levels in the HFD we are using now and diet can drive increases in FAHFA-TGs. In subsequent work, it will be of interest to investigate whether FAHFAs and FAHFA-TGs are co-regulated or differentially regulated in different metabolic states.

CONCLUSIONS

In this work, we report the discovery of a structurally novel class of triacylglycerols which contain a FAHFA in place of one of the three fatty acids. The discovery and characterization of FAHFA-TGs indicates the existence of an uncharacterized branch of endogenous lipid metabolism. This novel pathway is potentially involved in metabolic and inflammatory diseases because of the biological activities of FAHFAs. We found FAHFA-TG levels are markedly higher than FAHFA levels in adipose tissue, supporting the idea that FAHFA-TGs may serve as a depot for FAHFAs. Whether FAHFA-TGs themselves have additional roles in cell function remains to be elucidated. Furthermore, we observed that FAHFA-TG levels are reduced when DGAT1 and DGAT2 are inhibited, and FAHFA levels are increased when lipolysis is induced. These data suggest that the homeostasis between FAHFAs and FAHFA-TGs are enzymatically regulated. Even though there are similarities between the regulation of FAHFA/FAHFA-TG metabolism and fatty acid/regular TG metabolism, higher nonesterified FAHFAs have distinguishing insulin sensitizing and anti-inflammatory functions whereas increases in nonesterified fatty acids can be detrimental to cellular function. The differential effects of DGAT1/2 inhibitors on the synthesis of FAHFA-TGs and regular TGs also distinguish these two pools of TGs. Future experiments may investigate whether additional enzymes are involved in regulating the balance of FAHFA-TG synthesis and breakdown, and how they respond to different physiological and pathological metabolic status to eventually control the net effect of FAHFAs.

METHODS

Materials

Solvents for LC-MS analysis were purchased from Honeywell Burdick & Jackson. ¹³C₄-PAHSA, d₃₁-PAHSA, Atglistatin, and CAY10499 were purchased from Cayman Chemical. Inhibitors of DGAT1 (PF 04620110) and DGAT2 (PF 06424439) were purchased from Tocris Bioscience.

Animals

HFD fed C57BL/6 male mice were obtained from the Jackson Laboratory (Bar Harbor, ME; stock number 380050), and maintained on high fat diet (Research Diets, D12492) until the age of 36 weeks when they were sacrificed for tissue collection. Ad lib fed and fasted mice in C57BL/6 genetic background were bred in-house and were maintained on chow diet (RD, PicoLab 5053 Lab Diet). 10 week-old male mice were ad lib fed or fasted for 18 hours

before they were sacrificed for tissue collection. All mice were maintained on a 12 h light and dark cycle. All procedures involving mice were approved by the Institutional Animal Care and Use Committee (IACUC) of the Salk Institute for Biological Studies.

Syntheses of FAHFA-TGs and 12-OAHSA-CE

Syntheses of FAHFA-TGs and 12-OAHSA-CE are detailed in the Supporting Information along with the spectral characterization data.

Lipid Nomenclature

Synthetic FAHFA-TGs are annotated as the FAHFA moiety and the two regular fatty acyl moieties which are represented by the number of carbon atoms:number of double bonds in a sequence reflecting their sn positions linked to the glycerol. The three moieties are separated by a slash (/). Since the sn position of fatty acids cannot be determined by the mass spectrometry analysis, an underscore symbol () was used to annotate endogenous FAHFA-TGs²¹.

Lipid Extraction

Lipids were extracted based on the Bligh-Dyer method unless otherwise stated^{22–23}. In brief, for extraction from cells, the cell pellet was re-suspended in PBS, followed by addition of methanol and chloroform to make 1:1:2 PBS:methanol:chloroform solvent (v/v/v). The mixture was shaken vigorously for 30 s, vortexed for 15 s. For extraction from tissues, the sample was Dounce homogenized in 1:1:2 PBS:methanol:chloroform solvent on ice. An appropriate amount of internal standards were added to chloroform prior to extraction as indicated in each experiment. The resulted homogenate was centrifuged at 2200 g for 6 min at 4 °C. The bottom organic layer was collected and dried under a gentle stream of nitrogen.

3T3-L1 Cell Differentiation

3T3-L1 differentiation was performed as described previously²⁴. 3T3-L1 preadipocytes were maintained in DMEM with 10% bovine calf serum (BCS) at 37 °C in a humidified atmosphere of 10% CO₂ in air. Two days after the cells reach confluency (day 0), differentiation was induced by culturing the cells in DMEM containing 10% fetal bovine serum (FBS), 5 µg/ml insulin, 5 µM dexamethasone, and 0.1 mM IBMX. On day 2, the media were changed to DMEM with 10% FBS and 5 µg/ml insulin. Cells were fed every other day with the insulin-supplemented medium until days 8–10, when they are ready for treatment.

Incorporation of ¹³C₄-PAHSA, DGAT inhibition and quantification of ¹³C₄-PAHSA-containing triacylglycerols

Differentiated 3T3-L1 adipocytes were fed with 20 µM ¹³C₄-PAHSA or vehicle in phenol-free DMEM with 10% FBS for 24 hrs. For inhibition experiments, the cells were pretreated with 200 nM PF-04620110 (DGAT1 inhibitor) or/and PF-06424439 (DGAT2 inhibitor) for 30 minutes. Cells were washed twice with ice-cold PBS, harvested by scraping, and re-suspended in PBS. To determine protein concentration, a small aliquot of cell suspension was saved for Bradford assay. Lipid extraction was performed using the protocol described

above with 0.1 pmol of $^{13}\text{C}_{16}$ -PAHSA/16:0/16:0-TG and 0.15 pmol $^{13}\text{C}_{16}$ -PAHSA/16:1/16:0-TG added as internal standards. Lipid extract was reconstituted in 100 μl of methanol: chloroform solvent (1:2, v/v), and 10 μl was injected for LC-MS analysis on an Acquity UPLC system interfaced with a TSQ Quantiva mass spectrometer (Thermo Fisher Scientific). Lipids were separated on a Kinetex (Phenomenex) C18 column (2.6 μm , 150 \times 2.1 mm) over a 68-min gradient as follows: 0–70% B in 5 min, 70–85% B in 45 min, 85–100% B in 0.1 min, held at 100% B for 4.9 min, 100–0% B in 0.1 min, held at 0% B for 12.9 min. Solvent A was 64:40 methanol:water with 0.1% formic acid and 5 mM ammonium formate. Solvent B was 90:10 isopropanol:methanol with 0.1% formic acid and 5 mM ammonium formate. Flow rate was set to 0.1 ml/min at the beginning and ramped to 0.25 ml/min in 1 min. Multiple Reaction Monitoring (MRM) experiment was carried out in the negative ionization mode with the following ion source parameters: spray voltage, 3.4 kV; sheath gas, 15 L/min; aux gas, 7 L/min; sweep gas, 0 L/min; ion transfer tube temperature, 329 $^{\circ}\text{C}$; vaporizer temperature, 297 $^{\circ}\text{C}$. Q1 and Q3 resolution were both set to 0.7. $^{13}\text{C}_{16}$ -PAHSA/16:0/16:0-TG, $^{13}\text{C}_{16}$ -PAHSA/16:1/16:0-TG, and various $^{13}\text{C}_4$ -PAHSA-containing TG species were monitored. Their ammonium adducts were selected as the precursor ions. Simultaneous neutral loss of a fatty acyl group ($^{13}\text{C}_{16}$ -PAHSA/ $^{13}\text{C}_4$ -PAHSA, $^{13}\text{C}_{16}$ -PA/ $^{13}\text{C}_4$ -PA, or each of the other two acyls) plus ammonia were selected as the product ions. Collision energy and RF lens voltage were optimized using the two standards. The transition corresponding to the loss of $^{13}\text{C}_{16}$ -PAHSA or $^{13}\text{C}_4$ -PAHSA was used for quantification. Absolute quantification of $^{13}\text{C}_4$ -PAHSA-containing TGs was performed using $^{13}\text{C}_{16}$ -PAHSA/16:1/16:0-TG except that $^{13}\text{C}_4$ -PAHSA_16:0_16:0-TG was quantified using $^{13}\text{C}_{16}$ -PAHSA/16:0/16:0-TG. The results were normalized to protein concentration.

3T3-L1 Cell Lipolysis

Lipolysis was stimulated by incubating 3T3-L1 adipocytes for 2 hrs with 1 mM IBMX or 20 μM FSK in phenol-free DMEM containing 0.2% fatty acid free BSA. For inhibition experiments, cells were pre-treated with 10 μM Atglistatin or 0.1 μM CAY10499 for 2 hrs. Cells were washed twice with ice-cold PBS, scraped into PBS, and pelleted by centrifugation at 2000 g for 10 min at 4 $^{\circ}\text{C}$. Medium was collected and centrifuged at 5000 rpm for 10 min at 4 $^{\circ}\text{C}$. Lipids were extracted from cells and media with $^{13}\text{C}_4$ -PAHSA spiked in as the internal standard.

Quantification of nonesterified FAHFAs and TG-esterified FAHFAs

Frozen tissues of similar size were weighed and subjected to lipid extraction. $^{13}\text{C}_4$ -PAHSA was added for quantification of nonesterified FAHFAs in the lipid extract. $^{13}\text{C}_{16}$ -PAHSA/16:0/16:0-TG (sn1) or 16:0/ $^{13}\text{C}_{16}$ -PAHSA/16:0-TG (sn2) was added for quantification of FAHFA-TGs. The amount of internal standards were based on the tissue weight. Two rounds of solid-phase extraction (SPE) were performed as described previously⁸. Briefly, the silica cartridge (Strata SI-1, 500 mg silica, 3 mL, Phenomenex, 8B-S012-HBJ-T) was conditioned with 6 ml of hexane. Crude lipid extract normalized to tissue weight was loaded onto the column. Neutral lipids were eluted with 6 ml of 95:5 hexane:ethyl acetate. FAHFAs were subsequently eluted with 4 ml of ethyl acetate. This nonesterified FAHFA fraction was dried, reconstituted in 60 μl of methanol, and 10 μl was subjected to LC-MS analysis. The neutral lipid fraction was reconstituted in ethanol and treated with 20 μl of 1M LiOH at room

temperature for 24 hrs with constant shaking. At the end of the reaction, 20 μ l of 2 M HCl was added to neutralize the base. Lipids was extracted from the solution with 1 ml of PBS, 1 ml of ethanol, and 2 ml of chloroform with $^{13}\text{C}_4$ -PAHSA or d_{31} -PAHSA. A second SPE was performed to remove the remaining neutral lipids as they interfere with the FAHFA measurement. The resulting FAHFA fraction was collected for LC-MS analysis. Hydrolysis rate was calculated by dividing the amount of $^{13}\text{C}_{16}$ -PAHSA that is released from the $^{13}\text{C}_{16}$ -PAHSA-containing TG standard by the amount of the $^{13}\text{C}_{16}$ -PAHSA-containing TG standard. TG-esterified FAHFAs are then quantified by dividing the amount of FAHFA after hydrolysis by the hydrolysis rate.

Supplementary Material

Refer to Web version on PubMed Central for supplementary material.

ACKNOWLEDGMENT

We thank Dr. Matthew Kolar for helpful discussions and performing activity assay; Tina Chang for performing activity assay; Cynthia Donaldson for technical assistance.

Funding Sources

This work was supported by the National Institutes of Health Grants R01 DK043051 and P30DK57521 (to B. B. K.) and R01 DK106210 (to B. B. K. and A. S.), a grant from the JPB Foundation (to B. B. K.), Leona M. and Harry B. Helmsley Charitable Trust Grant 2012-PG-MED002 (to A. S.), Pioneer Fund (to D.T.), F32 DK111159 (M.E.E), the NCI Cancer Center Support Grant P30 (CA014195 MASS core, to A.S.), and Dr. Frederick Paulsen Chair/Ferring Pharmaceuticals (to A.S.).

ABBREVIATIONS

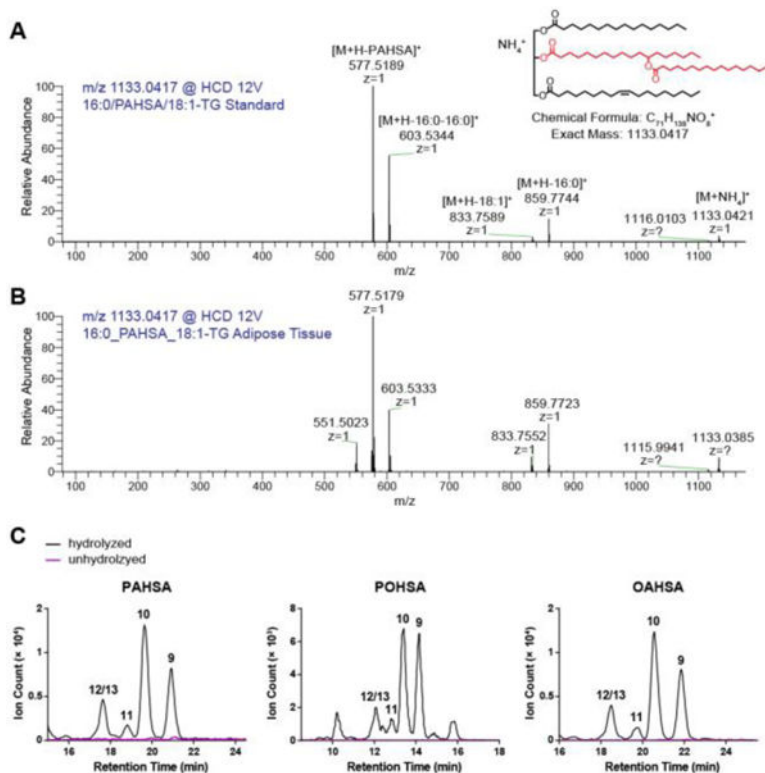
FAHFA	fatty acid ester of hydroxy fatty acid
PAHSA	palmitic acid ester of hydroxy stearic acid
POHSA	palmitoleic acid ester of hydroxy stearic acid
OAHSA	oleic acid ester of hydroxy stearic acid
FAHFA-TG	FAHFA-containing triacylglycerol
FAHFA-CE	FAHFA-containing cholesteryl ester
TG	triacylglycerol
CE	cholesteryl ester
DGAT	acyl-CoA:diacylglycerol acyltransferase
IBMX	3-isobutyl-1-methylxanthine
FSK	forskolin
Atgli	Atglistatin
CAY	CAY10499

PG-WAT	perigonadal white adipose tissue
SQ-WAT	subcutaneous white adipose tissue

REFERENCES

1. Shepherd PR; Gnudi L; Tozzo E; Yang H; Leach F; Kahn BB, Adipose cell hyperplasia and enhanced glucose disposal in transgenic mice overexpressing GLUT4 selectively in adipose tissue. *J Biol Chem* 1993, 268 (30), 22243–6. [PubMed: 8226728]
2. Yore MM; Syed I; Moraes-Vieira PM; Zhang T; Herman MA; Homan EA; Patel RT; Lee J; Chen S; Peroni OD; Dhaneshwar AS; Hammarstedt A; Smith U; McGraw TE; Saghatelian A; Kahn BB, Discovery of a class of endogenous mammalian lipids with anti-diabetic and anti-inflammatory effects. *Cell* 2014, 159 (2), 318–32. [PubMed: 25303528]
3. Carvalho E; Kotani K; Peroni OD; Kahn BB, Adipose-specific overexpression of GLUT4 reverses insulin resistance and diabetes in mice lacking GLUT4 selectively in muscle. *Am J Physiol Endocrinol Metab* 2005, 289 (4), E551–61. [PubMed: 15928024]
4. Kuda O; Brezinova M; Rombaldova M; Slavikova B; Posta M; Beier P; Janovska P; Veleba J; Kopecky J Jr.; Kudova E; Pelikanova T; Kopecky J, Docosahexaenoic acid-derived fatty acid esters of hydroxy fatty acids (FAHFAs) with anti-inflammatory properties. *Diabetes* 2016, 65 (9), 2580–90. [PubMed: 27313314]
5. Kuda O; Brezinova M; Silhavy J; Landa V; Zidek V; Dodia C; Kreuchwig F; Vrbacky M; Balas L; Durand T; Hubner N; Fisher AB; Kopecky J; Pravenec M, Nrf2-mediated antioxidant defense and peroxiredoxin 6 are linked to biosynthesis of palmitic acid ester of 9-hydroxystearic acid. *Diabetes* 2018, 67 (6), 1190–1199. [PubMed: 29549163]
6. Zhu QF; Yan JW; Zhang TY; Xiao HM; Feng YQ, comprehensive screening and identification of fatty acid esters of hydroxy fatty acids in plant tissues by chemical isotope labeling-assisted liquid chromatography-mass spectrometry. *Anal Chem* 2018, 90 (16), 10056–10063. [PubMed: 30052436]
7. Ma Y; Kind T; Vaniya A; Gennity I; Fahrman JF; Fiehn O, An in silico MS/MS library for automatic annotation of novel FAHFA lipids. *J Cheminform* 2015, 7, 53. [PubMed: 26579213]
8. Syed I; Lee J; Moraes-Vieira PM; Donaldson CJ; Sontheimer A; Aryal P; Wellenstein K; Kolar MJ; Nelson AT; Siegel D; Mokrosinski J; Farooqi IS; Zhao JJ; Yore MM; Peroni OD; Saghatelian A; Kahn BB, Palmitic acid hydroxystearic acids activate gpr40, which is involved in their beneficial effects on glucose homeostasis. *Cell Metabolism* 2018, 27 (2), 419–427 e4. [PubMed: 29414687]
9. Lee J; Moraes-Vieira PM; Castoldi A; Aryal P; Yee EU; Vickers C; Parnas O; Donaldson CJ; Saghatelian A; Kahn BB, Branched fatty acid esters of hydroxy fatty acids (FAHFAs) protect against colitis by regulating gut innate and adaptive immune responses. *Journal of Biological Chemistry* 2016, 291 (42), 22207–22217. [PubMed: 27573241]
10. Kolar MJ; Kamat SS; Parsons WH; Homan EA; Maher T; Peroni OD; Syed I; Fjeld K; Molven A; Kahn BB; Cravatt BF; Saghatelian A, Branched fatty acid esters of hydroxy fatty acids are preferred substrates of the mody8 protein carboxyl ester lipase. *Biochemistry* 2016, 55 (33), 4636–41. [PubMed: 27509211]
11. Parsons WH; Kolar MJ; Kamat SS; Cognetta AB 3rd; Hulce JJ; Saez E; Kahn BB; Saghatelian A; Cravatt BF, AIG1 and ADTRP are atypical integral membrane hydrolases that degrade bioactive FAHFAs. *Nat Chem Biol* 2016, 12 (5), 367–372. [PubMed: 27018888]
12. Listenberger LL; Han X; Lewis SE; Cases S; Farese RV Jr.; Ory DS; Schaffer JE, Triglyceride accumulation protects against fatty acid-induced lipotoxicity. *Proc Natl Acad Sci US A* 2003, 100 (6), 3077–82.
13. Zimmermann R; Strauss JG; Haemmerle G; Schoiswohl G; Birner-Gruenberger R; Riederer M; Lass A; Neuberger G; Eisenhaber F; Hermetter A; Zechner R, Fat mobilization in adipose tissue is promoted by adipose triglyceride lipase. *Science* 2004, 306 (5700), 1383–6. [PubMed: 15550674]
14. Yetukuri L; Soderlund S; Koivuniemi A; Seppanen-Laakso T; Niemela PS; Hyvonen M; Taskinen MR; Vattulainen I; Jauhiainen M; Oresic M, Composition and lipid spatial distribution of HDL particles in subjects with low and high HDL-cholesterol. *J Lipid Res* 2010, 51 (8), 2341–51. [PubMed: 20431113]

15. Zechner R; Zimmermann R; Eichmann TO; Kohlwein SD; Haemmerle G; Lass A; Madeo F, FAT SIGNALS--lipases and lipolysis in lipid metabolism and signaling. *Cell Metabolism* 2012, 15 (3), 279–91. [PubMed: 22405066]
16. Neises B; Steglich W, Simple method for the esterification of carboxylic acids. *Angew Chem Int Ed* 1978, 17 (7), 522–524.
17. McAnoy AM; Wu CC; Murphy RC, Direct qualitative analysis of triacylglycerols by electrospray mass spectrometry using a linear ion trap. *J Am Soc Mass Spectrom* 2005, 16 (9), 1498–1509. [PubMed: 16019221]
18. Murphy RC, Challenges in mass spectrometry-based lipidomics of neutral lipids. *TrAC Trends in Analytical Chemistry* 2018, 107, 91–98.
19. Murphy RC, Tandem mass spectrometry of lipids: molecular analysis of complex lipids. Royal Society of Chemistry: 2014.
20. Yen CL; Stone SJ; Koliwad S; Harris C; Farese RV Jr., Thematic review series: glycerolipids. DGAT enzymes and triacylglycerol biosynthesis. *J Lipid Res* 2008, 49 (11), 2283–301. [PubMed: 18757836]
21. Liebisch G; Vizcaino JA; Kofeler H; Trotschmuller M; Griffiths WJ; Schmitz G; Spener F; Wakelam MJ, Shorthand notation for lipid structures derived from mass spectrometry. *J Lipid Res* 2013, 54 (6), 1523–30. [PubMed: 23549332]
22. Bligh EG; Dyer WJ, A rapid method of total lipid extraction and purification. *Canadian Journal of Biochemistry and Physiology* 1959, 37 (8), 911–7. [PubMed: 13671378]
23. Zhang T; Chen S; Syed I; Stahlman M; Kolar MJ; Homan EA; Chu Q; Smith U; Boren J; Kahn BB; Saghatelian A, A LC-MS-based workflow for measurement of branched fatty acid esters of hydroxy fatty acids. *Nat Protoc* 2016, 11 (4), 747–63. [PubMed: 26985573]
24. Ertunc ME; Sikkeland J; Fenaroli F; Griffiths G; Daniels MP; Cao H; Saatcioglu F; Hotamisligil GS, Secretion of fatty acid binding protein aP2 from adipocytes through a nonclassical pathway in response to adipocyte lipase activity. *J Lipid Res* 2015, 56 (2), 423–34. [PubMed: 25535287]

**Figure 1.**

Discovery of FAHFA-TGs from adipose tissue of WT mice. High energy collisional dissociation (HCD) spectrum of m/z 1133.0417 corresponding to the ammonium adduct for 16:0/PAHSA/18:1-TG from (A) synthetic standard and (B) lipid extract of mouse adipose tissue. The shorthand notation of FAHFA-TGs is described in the method. (C) FAHFAs were detected after hydrolyzing a pool of triacylglycerols from adipose tissue under basic conditions that can cleave the ester bond to release the FAHFA from the FAHFA-TG. Shown are extracted ion chromatograms of three most highly upregulated FAHFA members in AG4OX mice—PAHSAs, POHSAs, and OAHSAs. The numbers above the peaks denote different regioisomers.

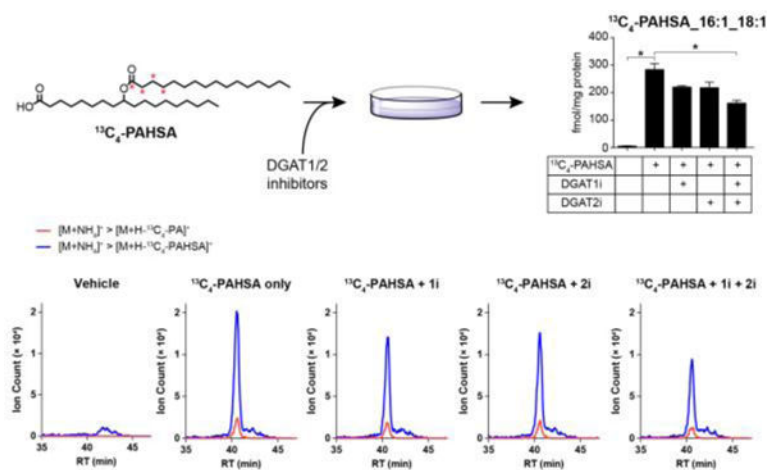


Figure 2. FAHFA-TGs can be synthesized in cells. $^{13}\text{C}_4$ -PAHSA-containing triacylglycerols were synthesized after incubating differentiated 3T3-L1 adipocytes with $20\ \mu\text{M}$ $^{13}\text{C}_4$ -PAHSA for 24 hours. The synthesis was inhibited by co-treating the cells with both DGAT1 inhibitor (1i) and DGAT2 inhibitor (2i). Shown is $^{13}\text{C}_4$ -PAHSA_16:1_18:1-TG level. $N = 3$, $*p < 0.05$, data are means \pm SEM. The bottom panel shows the extracted ion chromatograms of two transitions for $^{13}\text{C}_4$ -PAHSA_16:1_18:1-TG. Red curve, transition corresponding to the loss of $^{13}\text{C}_4$ -PA plus ammonia; Blue curve, transition corresponding to the loss of $^{13}\text{C}_4$ -PAHSA plus ammonia.

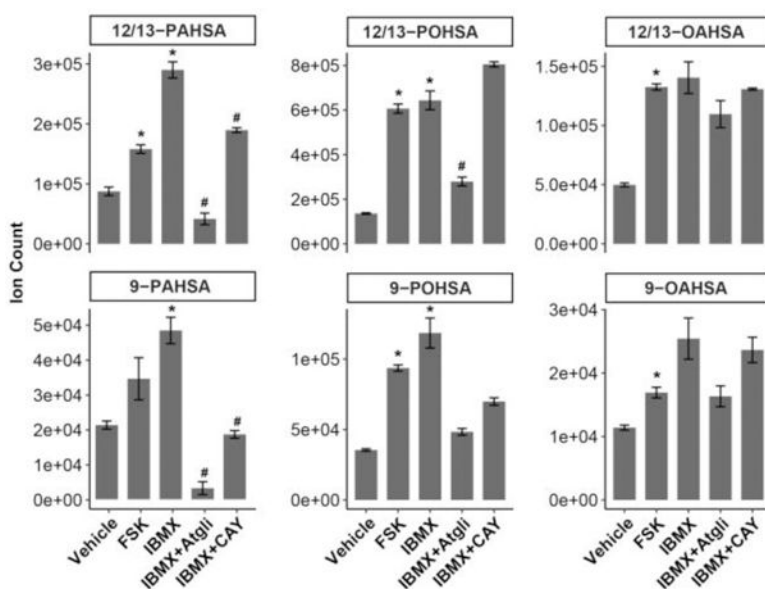


Figure 3.

FAHFA levels are regulated by lipolysis. FAHFA levels were increased when lipolysis was stimulated by FSK or IBMX in 3T3-L1 adipocytes. The ATGL inhibitor Atglistatin and the HSL-MAGL dual inhibitor CAY10499 reduced the effect of IBMX on FAHFA levels. N = 3, *p < 0.05 versus vehicle, #p < 0.05 versus IBMX, data are means ± SEM.

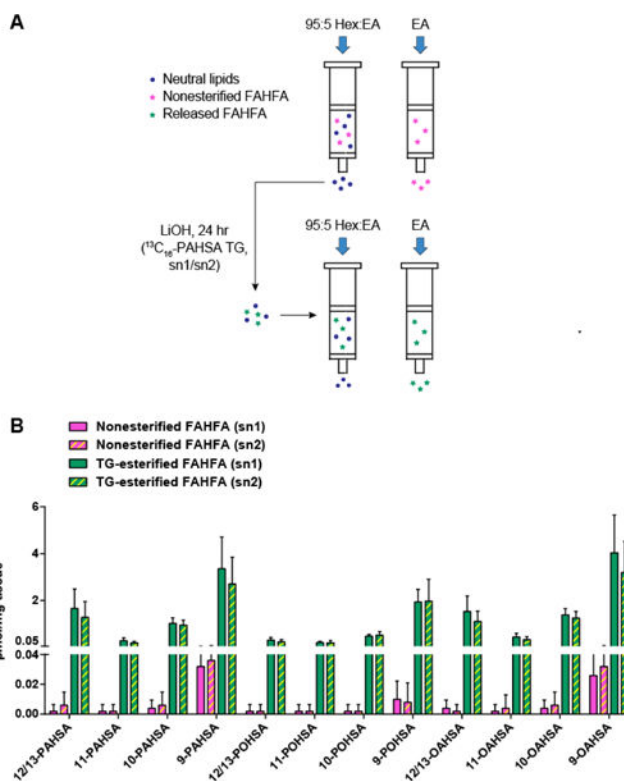


Figure 4. Quantification of FAHFA-TGs in adipose tissue of WT mice. (A) Workflow using a selective alkaline hydrolysis method. (B) Quantification of nonesterified and TG-esterified FAHFAs in SQ-WAT of WT mice. N = 5, data are means \pm SEM.

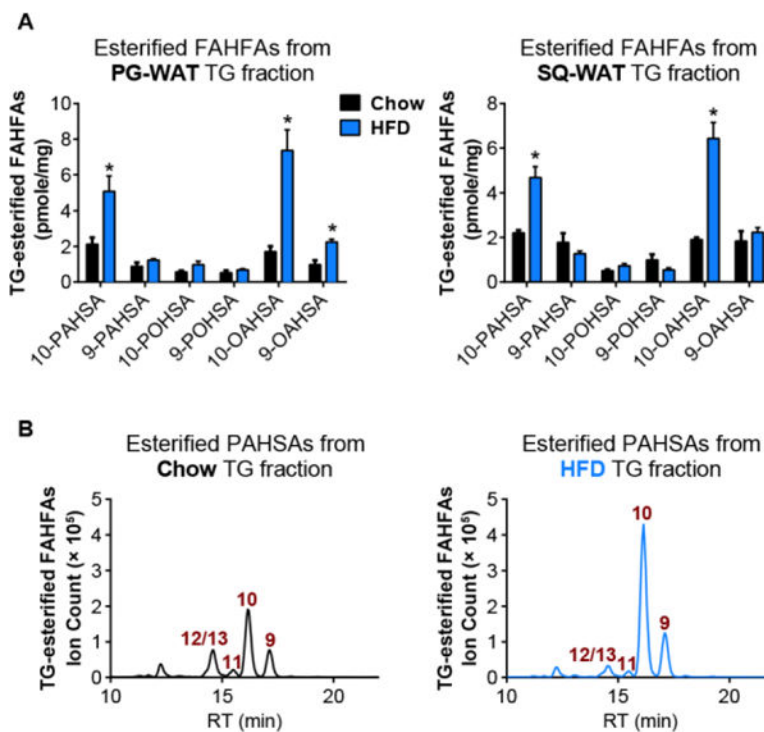
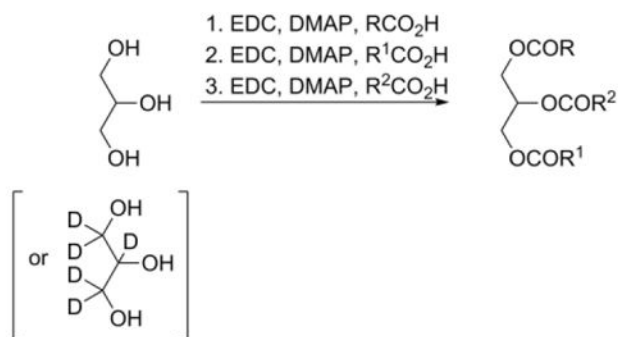
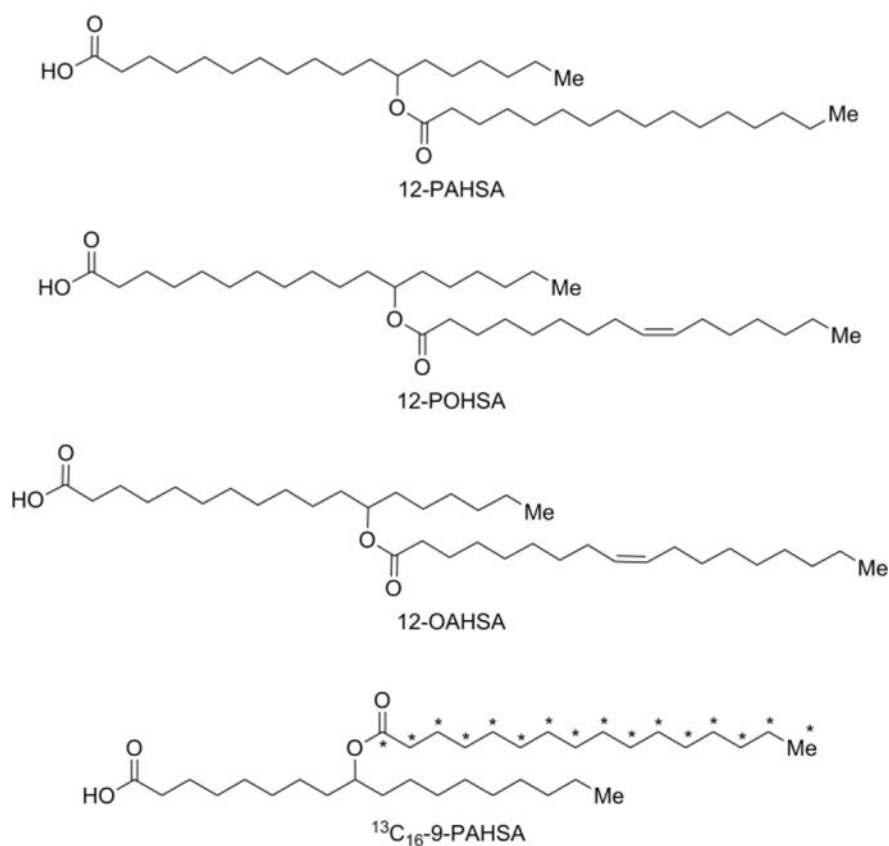


Figure 5. Measurement of TG-esterified FAHFAs reveals diet-induced changes in FAHFA-TG levels in WAT depots. (A) TG-esterified FAHFA levels in PG-WAT and SQ-WAT of WT mice on chow (black bars) or HFD (blue bars). N= 3–4, * $p < 0.05$, data are means \pm SEM. (B) Extracted ion chromatograms of TG-esterified 9-, 10-, 11-, and 12/13-PAHSAs in PG-WAT from chow (black) or HFD (blue) fed mice.



Fatty Acids: oleic, stearic, palmitic, and palmitoleic acid

FAHFAs:



Scheme 1.

Syntheses of FAHFA-based standards using iterative, modified Steglich esterification reactions^a

^aDMAP: 4-dimethylaminopyridine, EDC: i-ethyl-3-(3-dimethylaminopropyl)carbodiimide, PAHSA: palmitic acid ester of hydroxy stearic acid, POHSA: palmitoleic acid ester of hydroxy stearic acid, OAHSA: oleic acid ester of hydroxy stearic acid.